17th World Conference on Earthquake Engineering, 17WCEE

Sendai, Japan - September 13th to 18th 2020

DAMAGE LIMIT STATES FOR ARTISTIC ASSETS FROM CYCLIC AND DYNAMIC TESTS ON PLASTERED MASONRY WALLS

G. Guerrini(1), I. Senaldi(2), M. Tacci(3), A. Penna(4), K. Beyer(5), M. Rota(6)

(1) *Post-doctoral researcher, University of Pavia and EUCENTRE Foundation, Italy, gabriele.guerrini@unipv.it*
(2) *Post-doctoral researcher, University of Pavia and EUCENTRE Foundation, Italy, ilaria.senaldi@unipv.it*
(5) *Research engineer, EUCENTRE Foundation, Italy, matteo.tacci@eucentre.it*
(4) *Associate Professor, University of Pavia and EUCENTRE Foundation, Italy, andrea.penna@unipv.it*
(5) *Associate Professor, École Polytechnique Fédérale de Lausanne (EPFL), Switzerland, katrin.beyer@epfl.ch*
(6) *Researcher, EUCENTRE Foundation, Italy, maria.rota@eucentre.it*

Abstract

Recent earthquakes have dramatically demonstrated the consequences of the seismic vulnerability of cultural heritage assets worldwide. Nevertheless, this critical issue still needs to be fully explored, as earthquake engineering efforts have been mostly devoted to structural performance and life safety rather than to non-structural response and damage control in the past. The protection of artistic assets to seismic actions requires the identification of the main damage mechanisms and the definition of proper limit states depending on the different asset typology, which can be either movable (such as paintings and statues) or unmovable (e.g. frescos, stuccoes, pinnacles, and balconies).

Experimental tests conducted at the University of Pavia and at the EUCENTRE Foundation allowed investigating the correlation between the response of structural masonry walls and the damage to non-structural unmovable artistic assets attached to them. The testing campaign included in-plane quasi-static cyclic shear-compression tests on individual piers and shake-table tests on a half-scale building prototype. The specimens were constructed with double-leaf stone masonry made of undressed blocks and river pebbles. The walls were plastered on one side to simulate the presence of unmovable cultural heritage features.

The tested prototypes were monitored by potentiometers, accelerometers, and an optical acquisition system, that allowed monitoring the response of both structural and nonstructural elements. Different limit states of both masonry walls and attached plaster were defined based on the damage level recorded at each stage of testing. Analysis of the experimental results permitted correlating some engineering demand parameters, such as interstorey drift ratios and deformations of structural elements, to the damage extent identified on the plastered surfaces for each limit state of interest.

Keywords: cultural heritage assets, damage limit states, in-plane cyclic shear test, plaster, stone masonry

1. Introduction

Seismic risk assessment and mitigation related to historic and artistic assets plays an essential role in the preservation of cultural heritage worldwide. These assets include mainly non-structural components, which can be classified either as movable building contents (e.g. paintings and statues) or as unmovable elements attached to the structure (e.g. frescos, stuccoes, pinnacles, and balconies). However, earthquake engineering efforts have been mostly devoted to structural performance and life safety rather than to non-structural response and damage control, requiring further investigation of the seismic behavior of these components when subjected to seismic actions. Non-structural components are generally subjected to forced vibrations during seismic events, but elements attached to structural elements are also required to accommodate deformations induced by relative displacements on walls, floors, ceilings, or vaults. For these reasons, frescoes, stuccoes, and wall paintings are particularly vulnerable to seismic excitation in addition to aging effects. In fact, these ornaments are commonly obtained from brittle materials, with damage related to cracking and detachment from the structural support. The nature of the adhesive material (e.g. plaster) or the type of fastening adopted influence significantly their performance, as well as the deformability and crack-sensitivity of the structural masonry elements [1]. Moreover, floor and wall out-of-plane accelerations can affect the response of heavy protruding components.

The seismic vulnerability of plasters as non-structural components can be assessed implicitly, by studying the performance of the structural elements supporting artworks [2], or explicitly, by defining specific limit states for these components [3][4]. In the first case, a multi-scale approach can be adopted, starting from the global seismic analysis of the building, then moving to the local behavior of the subassemblies directly affecting the artwork, and finally focusing on micro-models of the structural elements supporting the heritage assets. Explicit damage limit states for plasters and, consequently, for frescoes or other wall paintings have been proposed by [3][4] in terms of interstorey drift ratios. These authors investigated the experimental behavior of plastered masonry walls and identified four non-structural damage states: A1, uncracked plaster detachment from the support; A2, plaster first visible cracking; A3, plaster extensive but repairable damage; A4, plaster fall and permanent loss. Empirical correlations between artistic assets limit states and structural limit states can result in reduction coefficients, which can be applied to the interstorey drift ratios associated with structural limit states to obtain those related to artistic assets limit states. Factors affecting these correlations may include interaction between plaster and masonry support, masonry typology, plaster characteristics, pre-existing detachments, aging and humidity effects.

This paper focuses on an experimental campaign conducted at the University of Pavia and at the EUCENTRE Foundation (Italy), which allowed investigating the correlation between the structural response of masonry buildings and the non-structural damage to unmovable artistic assets [5][6][7]. The specimens were constructed with double-leaf stone masonry made of undressed blocks and river pebbles, featuring traditional medieval construction details of the city of Basel (Switzerland). The walls were plastered on one side to simulate unmovable cultural heritage features. The study gravitated around a series of incremental dynamic shake-table tests on a half-scale building aggregate prototype [5][6], and included in-plane quasi-static cyclic shear-compression tests on individual half-scale piers [7] and complementary material characterization [8]. Damage limit states of both masonry walls and attached plaster were qualitatively defined in terms of visible damage. In particular, first cracking (A2) and partial fall (A4) were considered for the plaster. These limit states were then correlated to engineering demand parameters, such as interstorey drift ratios and deformations of structural elements, based on the damage recorded during the incremental quasi-static and dynamic tests.

2. In-plane cyclic shear-compression tests

2.1 Description of the specimens

In-plane cyclic shear-compression tests allow determining the behavior of masonry piers subjected to horizontal cyclic forces in their plane. In particular, information about damage evolution, lateral strength, stiffness, displacement/deformation capacity, and hysteretic energy dissipation can be obtained. Several

parameters affect the in-plane response of piers. Among others, material characteristics, element geometry, restraint conditions, and axial compression level are the most significant ones [9][10].

Four masonry piers were built during construction of the shake-table prototype for in-plane cyclic shear-compression tests, using the same materials, construction techniques, and scaling factors adopted for the half-scale building prototype [7]. A nominal thickness of about 300 mm was selected, which is the average thickness of the walls of the shake-table prototype. Walls were constructed in double-leaf undressed stone masonry (stone dimensions of about 100÷400 mm) with a 10%÷15% volume of river pebbles (diameter of about 50 mm). Stones were arranged in almost horizontal courses, although not perfectly regular given the variable dimensions of blocks and pebbles. Double-curvature conditions were imposed to the specimens, and two aspect ratios h/ℓ (i.e. ratio of pier height h to length ℓ) were selected: 1.26 for two squat piers CT02 and CT01 (Fig. 1a) and 3.0 for two slender piers CS01 and CS02 (Fig. 1b). For each aspect ratio, two axial compression levels σ_0/f_c (i.e. ratio of uniform normal stress σ_0 at the base to masonry compressive strength f_c) at the pier base were targeted: 0.2 and 0.3 for CT02 and CT01, and 0.3 and 0.45 for CS01 and CS02, respectively. One face of each pier was plastered, with a first leveling layer made of the same mortar used for the masonry (without EPS beads) and a 2-mm-thick skim coat [5].

Conducting tests on reduced scale specimens required a particular combination of scaling factors to avoid any alteration of accelerations or mass densities [5]. In this specific campaign, the masonry mechanical properties were reduced by the same geometrical scaling factor of 0.5, with respect to the masonry characteristics of reference, by selecting a suitable mortar composition constituted by a pre-mixed natural hydraulic lime mortar to which a 40% in volume of expanded polystyrene (EPS) beads was added. Vertical and diagonal compression test on masonry wallettes [7][8] determined the masonry mechanical properties, in particular mean Young's modulus E = 3460 MPa, Poisson's ratio υ = 0.14, shear modulus G = 1900 MPa, compressive strength f_c = 1.3 MPa, and tensile strength f_t = 0.17 MPa. The compressive strength of the half-scale specimens was compatible with the similitude relationships chosen for the dynamic test.

2.2 Test setup and protocol

The experimental setup for in-plane cyclic tests took advantage of the three-dimensional strong-walls/strong-floor configuration of the EUCENTRE laboratory [9][11]. Fundamental parts of this system were three servo-hydraulic actuators, with a maximum force capacity of 250 kN each and a stroke of 0.76 m. Two actuators applied an axial load to the specimen, while the third one imposed horizontal displacements to the top of the piers in the North-South direction (Fig. 2). Since a double-curvature configuration was chosen for the tests, vertical rotation of the pier top was prevented by the implementation of a hybrid control of the vertical actuators: they were forced to apply a constant total axial load and to maintain the same vertical displacement. Out-of-plane displacements of the pier top were prevented by specific restraints, allowing longitudinal translation only.

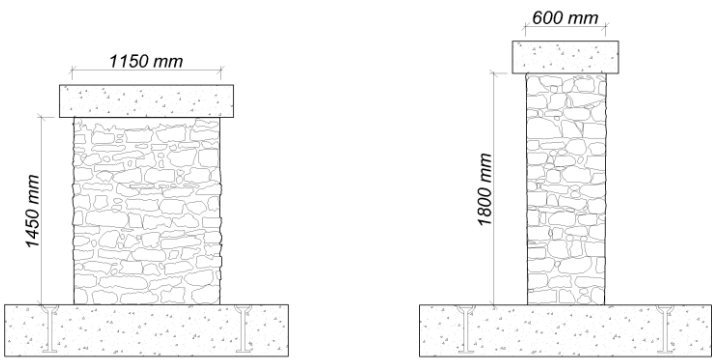

(a) (b)

Fig. 1 – In-plane cyclic shear-compression test specimens: (a) squat piers CT01 and CT02; (b) slender piers CS01 and CS02.

The specimens were densely instrumented with 28 displacement transducers, mounted on the non-plastered West face and on the North and South sides, to derive relative and absolute displacements and local deformations. A three-dimensional optical motion-capture system was instead employed on the plastered East face: passive retro-reflective spherical markers were glued to the pier surface and were monitored by fixed cameras recording their coordinates as they varied during the tests.

The first loading phase consisted of gradually applying the vertical load to the specimen in force control, until the target value was reached. Then, keeping the total vertical load constant, a rotation was imposed to the steel beam to compensate for the eccentricity of the horizontal actuator weight. Once equilibrium was established, with the vertical load centered on the masonry pier, the rotation of the steel beam was locked in for all subsequent testing phases.

In the following phase, the horizontal actuator was set in force control, and the pier was subjected to three push-and-pull cycles with force amplitude equal to 1/4 of its analytical shear strength and loading rate of 0.5 kN/s. This first sequence of loading was labeled 1F. The two following sequences of three cycles each, called 2F and 3F, were conducted either in force or displacement control, depending on the extent of nonlinearity observed on the recorded force-displacement response. Sequences 2F and 3F had amplitudes multiple of the lateral force or displacement reached in 1F, and loading rates of 0.5 kN/s or 0.025 mm/s. Finally, once a drift ratio $\theta = \delta/h$ (i.e. lateral top displacement δ normalized by the pier height h) of 0.05% was reached, a protocol consisting of displacement-controlled "D" sequences of increasing amplitude (Table 1) was followed. If the drift to be applied at sequence 1D was less than (or approximately equal to) those obtained for cycles 2F or 3F, those "F" cycles were skipped. The test was stopped if the specimen presented a potentially dangerous damage or a significant drop of lateral strength.

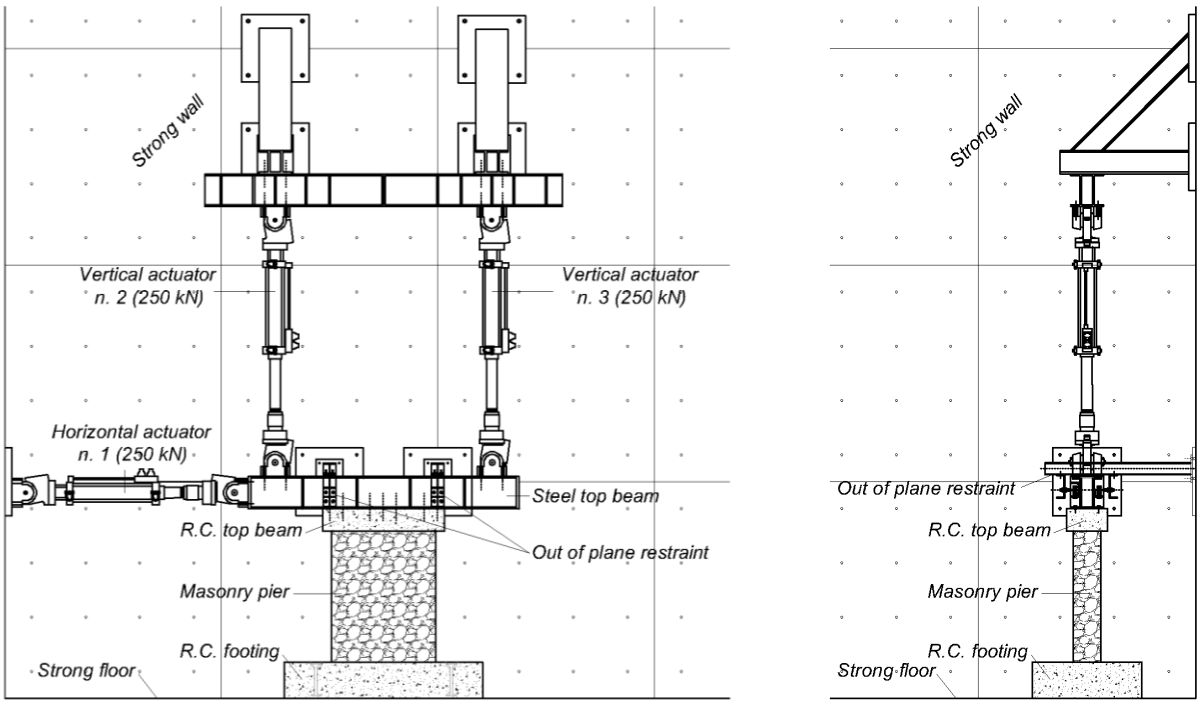

(a) (b)

Fig. 2 – In-plane cyclic shear-compression test setup: (a) front view; (b) side view.

Table 1 – In-plane cyclic shear-compression tests: displacement-controlled lateral loading sequences.

Sequence	CT01 and CT02		CS01 and CS02	
	Load rate [mm/s]	Drift ratio [%]	Load rate [mm/s]	Drift ratio [%]
1D	0.029	0.05	0.036	0.05
2D	0.035	0.075	0.043	0.075
3D	0.039	0.10	0.048	0.10
4D	0.044	0.15	0.054	0.15
5D	0.046	0.20	0.058	0.20
6D	0.058	0.25	0.072	0.25
7D	0.070	0.30	0.086	0.30
8D	0.093	0.40	0.115	0.40
9D	0.116	0.50	0.144	0.50
10D	0.139	0.60	0.173	0.60
11D	0.162	0.70	0.202	0.70
12D	0.186	0.80	0.230	0.80
13D	0.232	1.00	0.288	1.00
14D	0.290	1.25	0.360	1.25
15D	0.290	1.50	0.432	1.50
16D	0.290	1.75	0.576	2.00
17D	0.290	2.00	0.846	3.00
18D	0.348	3.00	1.152	4.00
19D	-	-	1.440	5.00

2.3 Test results

Drift ratios θ_{A2} and θ_{A4}, associated with non-structural damage states A2 and A4 respectively [3][4], were identified for each specimen. Moreover, drift ratios $\theta_{FC,F}$ and $\theta_{FC,S}$ at first structural cracking (damage state FC [3][4]) due to flexural and shear response respectively, and θ_{NC} at near-collapse conditions (damage state NC [3][4]), were also recorded. Flexural rocking behavior dominated specimens CT02 and CS01, whilst hybrid flexural-shear mechanisms were observed on the more heavily loaded piers CT01 and CS02.

Non-structural damage state A2 was attained in all specimens simultaneously with structural damage state FC due to flexure. Fist cracks appeared in the plastered surface of squat specimen CT01 at $\theta_{A2} = \theta_{FC,F} = 0.10\%$, with a horizontal crack extending for the entire length below the top stone course. For the other specimens, cracks originated at a corner below the top stone course at $\theta_{A2} = \theta_{FC,F} = 0.05\%$ for CT02, at $\theta_{A2} = \theta_{FC,F} = 0.15\%$ for CS01, and at $\theta_{A2} = \theta_{FC,F} = 0.10\%$ in the case of CS02. Fig. 3 depicts the crack patter of each pier at A2 damage state.

During cycles at peak drift ratio $\theta_{FC,S} = 0.3\%$, diagonal and vertical shear cracks started forming at the center of squat pier CT01 (Fig. 4). Increasing bulging was observed during the following sequence, and detachment and fall of plaster portions (damage state A4) occurred close to the shear-induced cracks during cycles at peak drift ratio $\theta_{A4} = 0.8\%$. Specimen CT01 reached near-collapse conditions at maximum drift ratio $\theta_{NC} = 1.75\%$, with diagonal shear failure accompanied by toe crushing at the base (Fig. 5). Slender pier CS02 attained non-structural damage state A4 at $\theta_{A4} = 1.0\%$, before shear cracking, when portions of plaster close to the top flexural crack detached and fell. Vertical and diagonal cracks started forming after reaching $\theta_{FC,S} = 1.5\%$, and progressive bulging was recorded (Fig. 4). At the end of the test ($\theta_{NC} = 3\%$), specimen CS02 exhibited simultaneous diagonal strut failure and toe crushing (Fig. 5), with stone expulsion from one bottom corner.

Flexure-dominated specimens CT02 and CS01 reached non-structural damage state A4 at $\theta_{A4} = 0.6\%$ and $\theta_{A4} = 1.25\%$ respectively, with portions of plaster falling from the top of the piers. Specimens CT02 and CS01 sustained maximum drift ratios $\theta_{NC} = 3.0\%$ and $\theta_{NC} = 5.0\%$, respectively, showing extensive toe crushing at structural limit state NC, although the squatter pier exhibited also sliding along the top and bottom horizontal rocking cracks (Fig. 5).

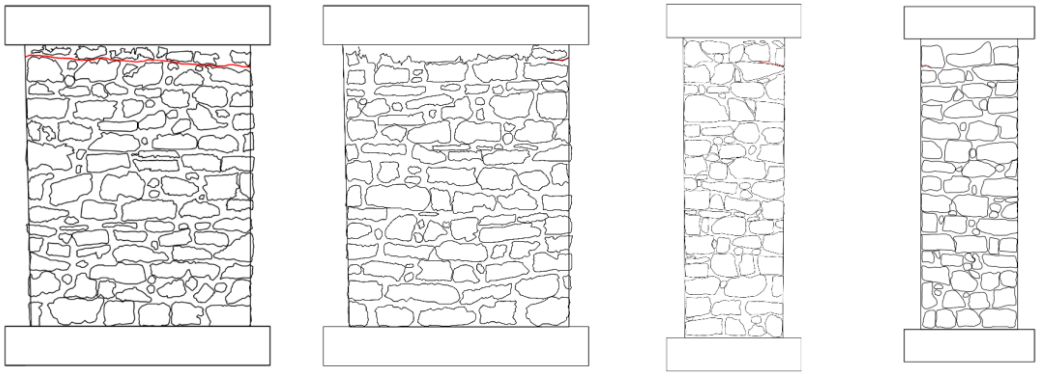

CT01	CT02	CS01	CS02
h/ℓ = 1.26	h/ℓ = 1.26	h/ℓ = 3.00	h/ℓ = 3.00
$\sigma_{0,bot}/f_c$ = 0.30	$\sigma_{0,bot}/f_c$ = 0.20	$\sigma_{0,bot}/f_c$ = 0.30	$\sigma_{0,bot}/f_c$ = 0.45
$\theta_{A2} = \theta_{FC,F} = 0.1\%$	$\theta_{A2} = \theta_{FC,F} = 0.05\%$	$\theta_{A2} = \theta_{FC,F} = 0.15\%$	$\theta_{A2} = \theta_{FC,F} = 0.1\%$

Fig. 3 – Damage conditions the four specimens at first cracking for flexural rocking.

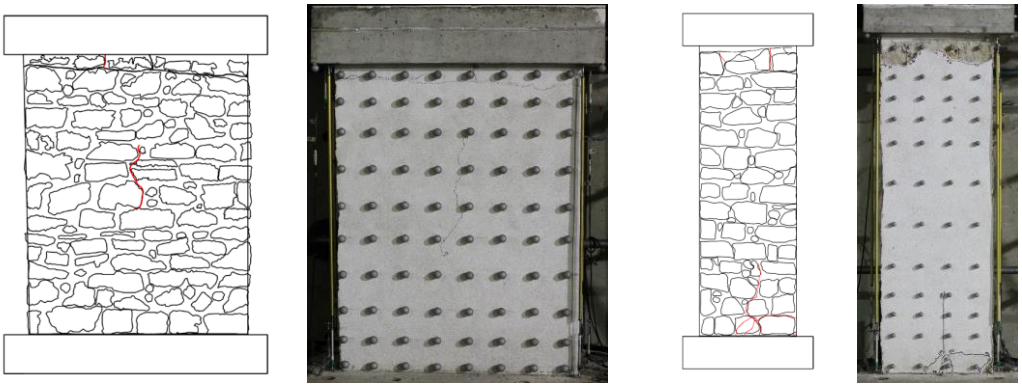

CT01	CS02
$h/\ell = 1.26$	$h/\ell = 3.00$
$\sigma_{0,bot}/f_c = 0.30$	$\sigma_{0,bot}/f_c = 0.45$
$\theta_{FC,S} = 0.3\%$	$\theta_{FC,S} = 1.5\%$

Fig. 4 – Damage conditions the CT01 and CS02 specimens with hybrid response.

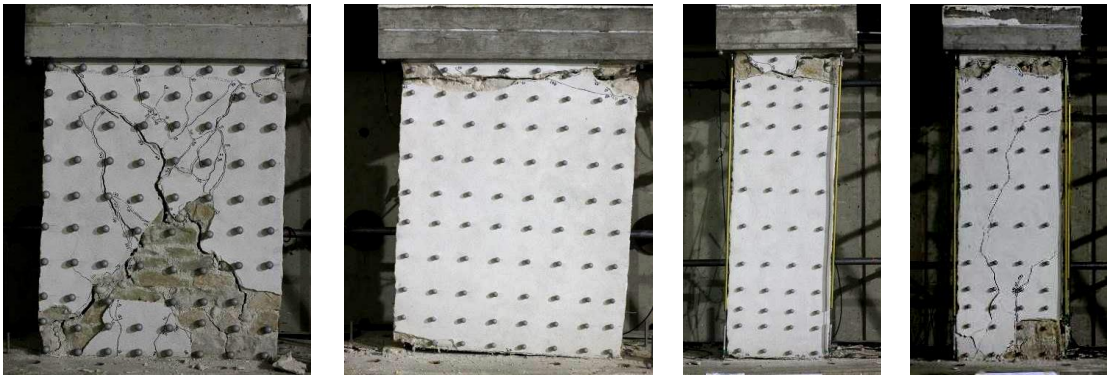

CT01	CT02	CS01	CS02
h/ℓ = 1.26	h/ℓ = 1.26	h/ℓ = 3.00	h/ℓ = 3.00
$\sigma_{0,bot}/f_c$ = 0.30	$\sigma_{0,bot}/f_c$ = 0.20	$\sigma_{0,bot}/f_c$ = 0.30	$\sigma_{0,bot}/f_c$ = 0.45
θ_{NC} = 1.75%	θ_{NC} = 3%	θ_{NC} = 5%	θ_{NC} = 3%

Fig. 5 – Damage conditions the four specimens at failure.

Table 2 – Artistic asset and structural drift values at different limit states

Pier	h/ℓ	$\sigma_{0,bot}/f_c$	θ_{A2}	θ_{A4}	$\theta_{FC,F}$	$\theta_{FC,S}$	θ_{NC}	Failure type
CT01	1.26	0.30	0.1%	0.8%	0.1%	0.3%	1.75%	Hybrid
CT02	1.26	0.20	0.05%	0.6%	0.05%	-	3.00%	Rocking
CS01	3.00	0.30	0.15%	1.25%	0.15%	-	5.00%	Rocking
CS02	3.00	0.45	0.10%	1.00%	0.10%	1.5%	3.00%	Hybrid

Table 2 summarizes the drift values associated with different damage states for plaster and structural masonry, from first cracking up to fall of plaster or structural near-collapse conditions. Drifts values at first cracking and fall of plaster are within the ranges identified by [4] for similar masonry typology and failure mechanisms.

3. Incremental dynamic shake-table tests

3.1 Description of the prototype

The prototype building aggregate included two adjacent three-story structural units (North and South), characterized by different roof heights, which shared a transverse party wall to emulate typical continuous façades along streets [5][6]. The West and the East façades were oriented parallel to the idealized street and to the chosen shaking direction. Because of the limited dimensions of the shake-table, the prototype was built at half-scale. The entire prototype (Fig. 6) was 5.8-m long and 5.6-m wide, constructed directly on composite steel-concrete footings bolted to the shake-table. The roof ridges were located 6.65 m and 7.6 m above the footings. The two structural units were weakly connected in correspondence of the transverse party wall, at its intersection with the East and West façades (Fig. 6), to simulate different construction periods. To create a weaker vertical joint between the units, a through-stone was provided across the joint only at every fourth course, alternatively in the external or internal leaf of the wall.

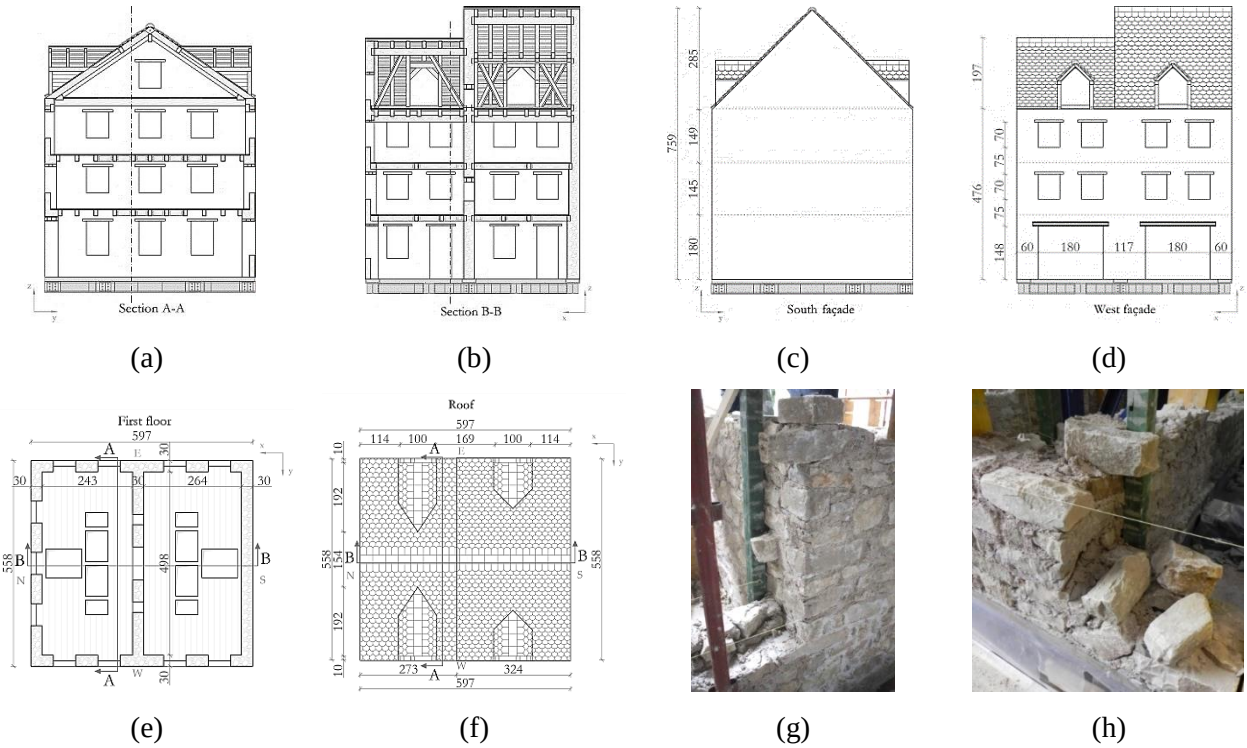

Fig. 6 – Building aggregate prototype: (a) section looking North; (b) section looking East; (c) South façade; (d) West façade; (e) first-floor plan; (f) roof plan; (g, h) structural joint connection detail.

All walls were constructed in double-leaf undressed stone masonry, with stones arranged in nearly horizontal courses, as illustrated for the in-plane shear-compression test specimens. Through stones were located only in correspondence of openings and corners. The masonry thickness varied along the height of the building, starting from 350 mm at the first story, decreasing to 300 mm at the second one, and ending with 250 mm at the third and attic stories. Only the party wall had constant 300-mm thickness from the base through the roof ridge. The mechanical properties of the masonry were the same as discussed for the four pier specimens, because the aggregate prototype and the piers were built at the same time and with the same materials [7][8]. Plaster was applied: (i) over the entire exterior surface of the East façade; (ii) over a strip across the structural joint; and (iii) the interior surface of two walls of the South unit at the first story.

Timber floor and roof framing provided flexible diaphragm to the building aggregate [5][6]. The timber floors of the prototype consisted of timber joists (typical section of 100x160 mm) and 20-mm-thick planks, nailed to the joists (Fig. 7a). The joists of the first and the second floors were oriented along the longitudinal shaking direction. Roof timber trusses (Fig. 7b) were oriented in the transverse direction and rested on 100x200-mm timber spreader beams, located atop the East and the West walls and embedded into the masonry thickness. Tile battens supporting clay tiles were directly nailed above the rafters, without any planks (Fig. 7c). The roof structures were characterized by slopes of 34° and 45° for the North and South units, respectively, and consequently by two different truss configurations. The shortest truss had a simple layout, without any king post or webs, while the steepest one was more complex with a collar tie beam and a supporting secondary structure. Diagonal braces were provided to increase the in-plane stiffness of the roof pitches.

(a) (b) (c)

Fig. 7 – Building aggregate prototype: (a) timber floor framing; (b) timber roof trusses with 45° slope; (c) tile battens and dormers.

3.2 Test protocol and instrumentation

Three natural accelerograms were selected to simulate increasing levels of shaking intensity [5][6]. The first two input signals were recently recorded in Switzerland: the signal "BAS" (PGA of 0.71 m/s^2) was recorded by a station in Basel, while the record "LIN" (PGA of 0.85 m/s^2) comes from a magnitude M_w 4.7 event occurred in the Linthal valley in March 2017. The "MON" input motion (PGA of 2.20 m/s^2) was recorded at the Ulcinj station during the 1979, M_w 6.9 Montenegro earthquake and is spectrum-compatible with the 475-years design displacement spectrum of the city of Basel [12][13][14], over a period range representative of masonry buildings. The digitization time step of all records was scaled by a factor 0.707, equal to the square root of the geometric scale factor of 0.5, to meet similitude laws [5].

The incremental dynamic test sequence was obtained by gradually increasing the acceleration amplitude of the ground motion [5][6]. The earthquake tests were alternated by random noise and calibration tests, performed at low intensity to calibrate the table controller and to identify dynamic properties evolution under progressive damage. Table 3 summarizes the sequence of main shocks imposed to the building specimen. The structural response of the prototype was monitored by a dense distribution of instruments [5]. The instrumentation consisted in 72 linear potentiometers, 16 wire potentiometers, 41 accelerometers and a 3D optical acquisition system monitoring the trajectories of spherical passive reflector markers attached to three façades, with the exception of the East wall.

Table 3 – Incremental dynamic test: input ground motion sequence.

Test #	Signal	Acceleration scale factor [%]	Recorded PGA [g]
10	BAS	100	0.0524
16	LIN	100	0.0529
19	MON	25	0.047
21	MON	50	0.098
26	MON	75	0.174
29	MON	100	0.204
33	MON	125	0.269
37	MON	150	0.321
42	MON	175	0.347

3.3 Test results

The prototype exhibited the first minor cracks (damage state FC[3][4]) after test MON-175% (PGA = 0.174 g) but did not affect the plaster. In fact, they were localized at the supports of the steel lintels of the large first-story openings and at the base of the South pier of the West façade (Fig. 8), which underwent an interstorey drift ratio θ_{FC} = 0.11%. The plastered surfaces reached damage state A2 [3][4] during test MON-100% (PGA = 0.204 g), when almost all spandrels of both longitudinal façades developed flexural, shear, or hybrid cracks (Fig. 9). Moreover, cracks formed around the timber lintels and at the roof truss supports. The maximum interstorey drift ratio θ_{A2} varied between 0.08% and 0.19%, depending on the location on the East and West façades. Structural and non-structural damage progressed into state A3 [3][4] during the following test runs, and after MON-150% limited portion of skim coat started flaking off from the timber lintels and close to the largest structural cracks.

During test MON-175% (PGA = 0.347 g) the building specimen reached a severe level of damage and was deemed approaching near-collapse conditions (damage state NC [3][4]), with interstorey drift ratios θ_{NC} between 0.62% and 1.54%. Significant residual crack widths and activation of out-of-plane overturning mechanisms of the North and South walls were observed. Floor joists pulled out from the North and South walls by a maximum of approximately 2.9 mm and 5.9 mm at the first and second floors, respectively, with residuals of about 2.2 mm and 4.6 mm. Flexural-rocking mechanisms occurred at the base of the piers of the East and West longitudinal façades, with elongation and widening of pre-existing cracks. At this stage of testing, portions of plaster and some stones completely detached from the masonry, at the top of the structural joint of the East façade, and were kept from falling only by instruments and cables: this meant that non-structural damage state A4 [3][4] had been reached, with a local interstorey drift ratio θ_{A4} = 1.12%.

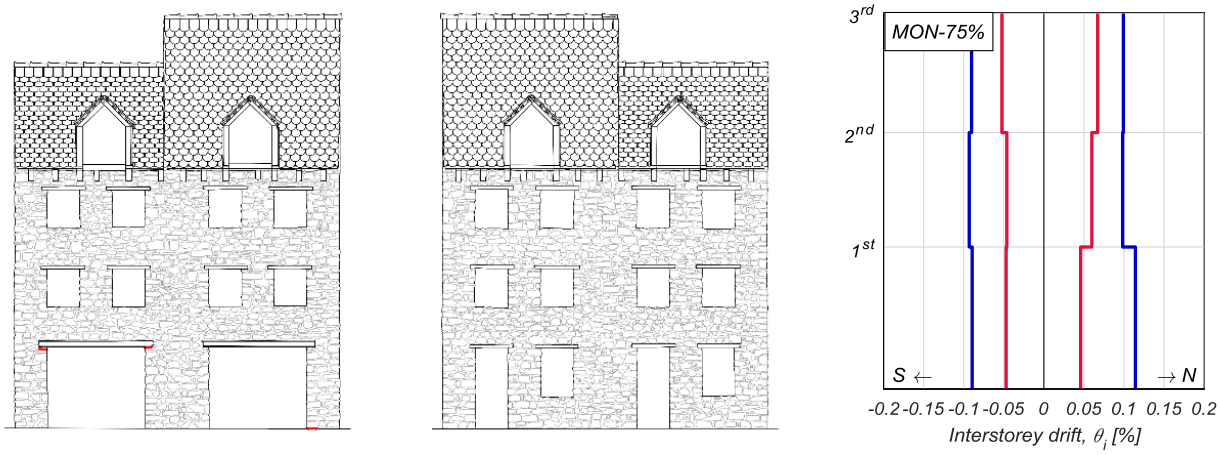

(a) (b) (c)

Fig. 8 – Results after test with PGA of 0.174 g: (a) West wall crack pattern; (b) East wall crack pattern; (c) interstory drift envelopes, West wall in blue and East wall in red.

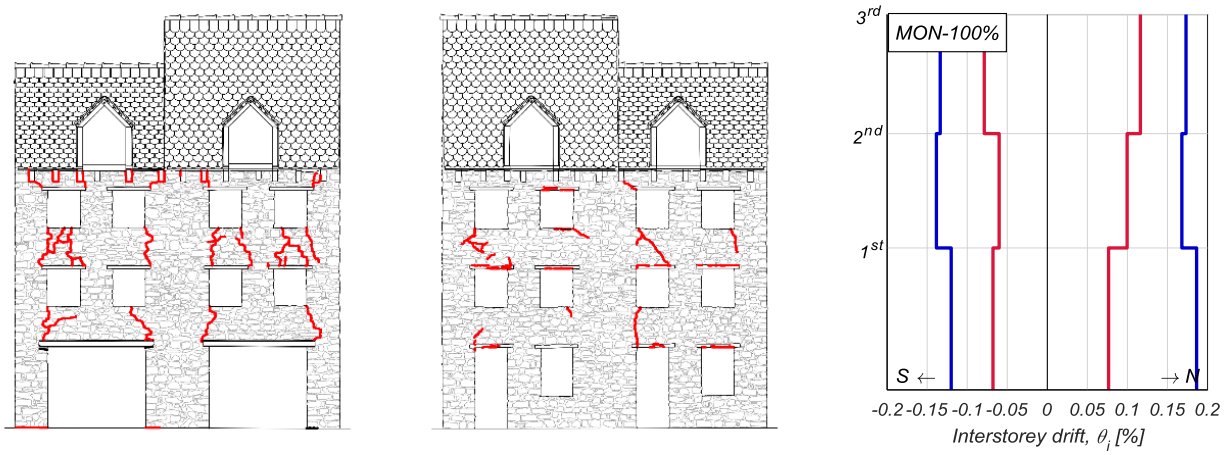

(a) (b) (c)

Fig. 9 – Results after test with PGA of 0.204 g: (a) West wall crack pattern; (b) East wall crack pattern; (c) interstory drift envelopes, West wall in blue and East wall in red.

(a) (b) (c)

Fig. 10 – Test results after MON-175% with PGA of 0.347 g: West wall fallen stone; (b) East wall completely detached stones and plaster; (c) interstory drift envelopes, West wall in blue and East wall in red.

4. Conclusions

In-plane cyclic shear-compression tests and incremental dynamic tests were performed on four half-scale stone-masonry piers and one building aggregate, to investigate the interaction between structural masonry and plaster and to identify non-structural and structural damage limit states.

The four piers were characterized by two aspect ratios and two axial compression levels. Their lateral response was dominated by flexure under lower axial compression for both aspect ratios, even though the squatter pier exhibited also sliding along the top and bottom horizontal rocking cracks. The heavily loaded pier displayed a hybrid failure mechanism, beginning with a flexural mode and transitioning towards a diagonal shear failure.

Plaster started cracking at drift ratios between 0.05% and 0.15% together with flexural cracking at the top of the piers. Fall of plaster was recorded instead for drift ratios between 0.6 % and 1.25%. Comparable

values of interstorey drift ratios for the same non-structural damage limit states were recorded during the incremental shake-table tests performed on the half-scale stone masonry building aggregate. Although measured on scaled specimens, the drift ratios at first cracking and at fall of plaster were within the ranges found in literature for full-scale piers subjected to in-plane cyclic shear-compression tests.

In rocking-dominated piers the loss of plaster occurred only at the top and bottom extremities of the panel. In piers with hybrid flexural-shear behavior, instead, shear deformation and cracking determined extensive damage with wide cracks (from 5 to 10 mm) and fall of plaster also in the center of the pier, where decorations and frescoes with high artistic value are likely to be located.

5. Acknowledgements

The work presented is part of the research project "Seismic assessment of natural stone masonry buildings in Basel - A research and training project", jointly carried by the École Polytechnique Fédérale de Lausanne and the University of Pavia, which was funded by the Swiss Federal Office for the Environment and the Construction Department of the Canton Basel-Stadt. Financial support to the data processing was also contributed by the EUCENTRE Foundation, within the project Mobartech (Regione Lombardia). The authors would like to thank Mapei S.p.a. for its support to the project. The help provided by M. Caruso, P. Comini, F. Dacarro, F. Di Santo, S. Girello, F. Graziotti, L. Grottoli, M. Mandirola, B. Marchesi, M. Tacci, and U. Tomassetti is gratefully acknowledged.

6. References

[1] Perrone D, Calvi PM, Nascimbene R, Fischer EC, Magliulo G (2019). Seismic performance of non-structural elements during the 2016 Central Italy earthquake. *Bulletin of Earthquake Engineering*, **17**(10), 5655-5677. DOI: 10.1007/s10518-018-0361-5

[2] Castori G, Borri A, De Maria A, Corradi M, Sisti R (2017). Seismic vulnerability assessment of a monumental masonry building. *Engineering Structures*, **136**, 454-465. DOI: 10.1016/j.engstruct.2017.01.035

[3] Calderini C, Degli Abbati S, Cotič P, Kržan M, Bosiljkov V (2015). In-plane shear tests on masonry panels with plaster: correlation of structural damage and damage on artistic assets. *Bulletin of Earthquake Engineering*, **13**(1), 237-256. DOI: 10.1007/s10518-014-9632-y

[4] Kržan M, Gostič S, Cattari S, Bosiljkov V (2015). Acquiring reference parameters of masonry for the structural performance analysis of historical buildings. *Bulletin of Earthquake Engineering*, **13**(1), 203-236. DOI: 10.1007/s10518-014-9686-x

[5] Senaldi I, Guerrini G, Comini P, Graziotti F, Penna A, Beyer K, Magenes G (2020). Experimental seismic performance of a half‐scale stone masonry building aggregate. *Bulletin of Earthquake Engineering*, **18**(2), 609-643. DOI: 10.1007/s10518-019-00631-2

[6] Guerrini G, Senaldi I, Graziotti F, Magenes G, Beyer K, Penna A (2019). Shake-table test of a strengthened stone masonry building aggregate with flexible diaphragms. *International Journal of Architectural Heritage*, **13**(7), 1078-1097. DOI: 10.1080/15583058.2019.1635661

[7] Senaldi I, Guerrini G, Scherini S, Morganti S, Magenes G, Beyer K, Penna (2018). Natural stone masonry characterization for the shaking-table test of a scaled building specimen. *Proc. 10th International Masonry Conference*, Milan, Italy.

[8] Guerrini G, Senaldi I, Scherini S, Morganti S, Magenes G, Beyer K, Penna A (2017). Material characterization for the shaking-table test of the scaled prototype of a stone masonry building aggregate. *Proc. 17th ANIDIS Conference*, Pistoia, Italy.

[9] Magenes G, Penna A, Galasco A, Da Parè M (2010). In-plane cyclic shear tests of undressed double-leaf stone masonry panels. *Proc. 8th International Masonry Conference*, Dresden, Germany.

[10] Magenes G and Calvi GM (1997). In-plane seismic response of brick masonry walls. *Earthquake Engineering and Structural Dynamics*, **26**(11), 1091-1112. DOI: 10.1002/(SICI)1096-9845(199711)26:11<1091::AID-EQE693>3.0.CO;2-6

[11] Magenes G, Morandi P, Penna A (2008). *Test results on the behaviour of masonry under static cyclic in plane lateral loads.* Research report RS-01/08, Department of Structural Mechanics, University of Pavia, Italy.

[12] SIA 261 (2014). *Einwirkungen auf Tragwerke*. Swiss Society of Engineers and Architects, Zurich, Switzerland (in German).

[13] Fäh D, Wenk T (2009). *Mikrozonierung für die Kantone Basel Stadt und Basel Landschaft, Optimierung der Form der Antwortspektren und der Anzahl der Mikrozonen*. Report, Swiss Seismological Service, ETH, Zurich, Switzerland (in German).

[14] Wenk T, Fäh D (2012). Seismic microzonation of the Basel area. *Proc. 15th World Conference on Earthquake Engineering*, Lisbon, Portugal.

